spheres, the spherical representation was used *only* to test for contacts; when evaluating the free energy of contacts (as in Figure 3 of ref 3), the spherical representation was abandoned, and the earlier form[24] of the data of Table III was used.[3]

(24) In our earlier calculations,[3] we used numerical values of $\Delta G°_{k,l}$ that were evaluated on the basis of a different definition from that described in section II of this paper (but using the same values of $N_{(n)k}$ and $N_{k,l}$ given in Table II). Therefore, the effect of this altered definition of $\Delta G°_{k,l}$ on the previous results[3] was checked. It was found that the general appearances of the contact regions in steps B and C are the same, but the precise locations of the contacts within each region and the type of contact (represented by numerals in the squares on the contact maps of Figures 4 and 5 of ref 3) are altered somewhat. Thus, the most important implication, discussed in the last paragraph of ref 3, is unchanged. The main reason for this is that both the old and the new sets of values of $\Delta G°_{k,l}$ reflect the general tendencies for strong contacts between nonpolar residues and for exposure of polar ones to the solvent.

(25) G. Nemethy, I. Z. Steinberg, and H. A. Scheraga, *Biopolymers*, **1**, 43 (1963).

(26) S. Tanaka and H. A. Scheraga, work in progress.

(27) S. Tanaka and H. A. Scheraga, *Macromolecules*, **8**, 494 (1975).

(28) S. Tanaka and A. Nakajima, *Macromolecules*, **5**, 708, 714 (1972).

Conformational Analysis of Poly(dihalophosphazenes)[1,2]

H. R. Allcock,* R. W. Allen, and J. J. Meister

Department of Chemistry, The Pennsylvania State University,
University Park, Pennsylvania 16802. *Received September 26, 1975*

ABSTRACT: The poly(dihalophosphazenes), $(NPF_2)_n$, $(NPCl_2)_n$, and $(NPBr_2)_n$, have been examined by conformational analysis using nonbonding intramolecular interactions based on a 6:12 Lennard-Jones potential and a Coulombic term. The results provide an insight into the reasons for the low glass transition temperatures, the high chain flexibilities, and the conformational preferences of these molecules.

High molecular weight polyphosphazenes, of general formula I, have physical properties that are unusual and, in many cases, unexpected.[3-16] The three halogeno derivatives, $(NPF_2)_n$, $(NPCl_2)_n$, and $(NPBr_2)_n$, are rubbery, elastomeric materials over a broad temperature range. For the fluoro derivative the elastomeric properties are maintained from the glass transition at −95 to +270 °C.[12] The corresponding rubbery range for the chloro derivative is from −63 to +350 °C and for the bromo compound from −15 to +270 °C. The methoxy and ethoxy derivatives,[3,4] $[NP(OCH_3)_2]_n$ and $[NP(OC_2H_5)_2]_n$, are flexible, film-forming materials with glass transition temperatures near −80 °C. These facts suggest that the polyphosphazene backbone has an unusually high torsional mobility.

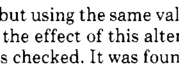

I

The conformational properties of polyphosphazenes are also unusual. The polymers, $[NPCl_2]_n$, $[NP(OCH_2CF_3)_2]_n$, $[NP(OCH_2C_3F_5)_2]_n$, $[NP(OC_6H_5)_2]_n$, and $[NP(OC_6H_4Cl\text{-}p)_2]_n$, crystallize when oriented. The x-ray diffraction patterns suggest a chain repeating distance of ~4.9 Å which can be rationalized in terms of a cis-trans planar arrangement (II).[3,4,17-19] On the other hand, poly(difluorophosphazene), $(NPF_2)_n$, shows two different x-ray patterns, one at temperatures between 25 and −36 °C, indicative of a 6.45 Å chain repeat, and the other at temperatures below −56 °C, with a 4.86 Å repeat distance and a cis-trans planar conformation.[12] The bromo derivative crystallizes only with difficulty,[19] but similarities have been reported between the x-ray patterns of $(NPBr_2)_n$ and $(NPCl_2)_n$.[20] It was of some interest to deduce the reasons for these conformational characteristics.

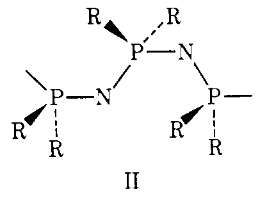

II

In this paper we have attempted to explain these experimental facts with the use of nonbonding intramolecular potential energy calculations. This paper deals with the three simplest systems, $(NPF_2)_n$, $(NPCl_2)_n$, $(NPBr_2)_n$, and the yet unsynthesized $(NPI_2)_n$. The accompanying paper considers organo-phosphazene polymers.

Model and Method

The Model. Two structural alternatives were employed which made use of the short chain segments shown in III and IV for calculation of the nonbonding interactions for independent incremental torsion of bonds P_1–N_2, N_2–P_2, P_2–N_3, and N_3–P_3. The initial position for the computations was the trans-trans conformation, shown in III and IV.

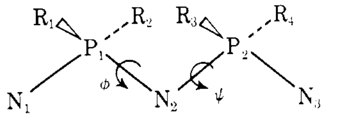

III

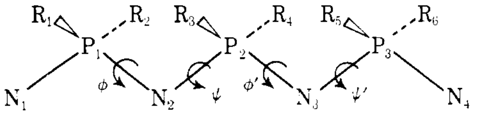

IV

The choice of bond angles and bond lengths was based on an analysis of published x-ray crystallographic data for cyclic trimers, tetramers, a pentamer,[21-28] and, in the case of $(NPF_2)_n$, the high polymer.[12] It was recognized that the restrictions imposed by six- or eight-membered ring structures could modify the preferred skeletal angles or interatomic distances. Therefore, trial models were used that explored changes in bond angles or bond lengths for values above and below those found for the small molecules. Table I lists the structural parameters used. The comprehensive background of crystallographic data for cyclic phosphazenes indicates that all the P–N bonds should be of equal length when only one type of R group is present.[21]

For structure III, the coordinate calculation programs computed intramolecular distances between the atoms for 10° incremental torsion of bonds P_1–N_2 and N_2–P_2 through 360°. Structure III was considered a nine-body problem, with neglect of those interactions, such as N_1–R_1, R_2–N_2, P_1–P_2, etc.,

Table I
Bond Angles and Bond Lengths Used in the Model Structures[a]

Polymer	N–P–N, deg	P–N–P, deg	R–P–R, deg	P–N, Å	P–R, Å
$(NPF_2)_n$	119 ($119^{b,22}$–$123^{c,23}$)	136 ($136^{e,12}$–$147^{c,23}$)	95 ($95^{e,12}$–$100^{c,23}$)	1.52 ($1.52^{e,12}$–1.60)	1.47 ($1.47^{e,12}$–$1.52^{b,22}$)
$(NPCl_2)_n$	118 ($118^{b,d,24,26}$–$119^{e,f,18}$–$121^{c,25}$)	130 ($120^{c,25}$–$127^{e,f,18}$–$149^{d,26}$–155)	$102^{d,26}$	1.52 ($1.52^{d,26}$–$1.56^{c,25}$–1.60)	$1.99^{b,c,24,25}$
$(NPBr_2)_n$	117 ($116^{b,27,28}$–118)	130 (124–140)	$103^{b,27,28}$	1.57 ($1.53^{b,27,28}$–$1.60^{b,27,28}$)	$2.18^{b,27,28}$
$(NPI_2)_n$[g]	120	130 (120–150)	103^{29}	1.60 (1.60–1.70)	2.48^{29}

[a] The values in parentheses indicate the range of values tested in trial calculations. [b] Value from cyclic trimer data. [c] From cyclic tetramer. [d] From cyclic pentamer. [e] From high polymer data. [f] Derived from optical transform analysis and, hence, less reliable than other x-ray data. [g] This polymer has not yet been synthesized. The values in ref 29 are from P_2I_4.

Table II
Interaction Parameters for Use in the Lennard–Jones Equation[a,b]

Interaction (I···J)	$A(1)_{ij}$	$B(1)_{ij} \times 10^{-4}$	$A(2)_{ij}$	$B(2)_{ij} \times 10^{-4}$
P···P	1473.0	170.7	3193.0	480.7
P···N	733.3	35.44	1323.0	132.4
N···N	362.9	16.09	548.3	35.40
P···F	446.5	29.04	580.9	50.70
P···Cl	1512.0	153.7	2823.0	392.6
P···Br			4060.0	661.1
P···I			5791.0	1151.0
N···F	222.4	4.755	241.4	13.45
N···Cl	738.8	37.31	1171.0	107.6
N···Br			1683.0	183.2
N···I			2400.0	323.2
F···F	134.6	3.652	119.5	5.727
Cl···Cl	1562.0	200.5	2515.0	322.6
Br···Br			5185.0	912.2
I···I			10510.0	2722.0

[a] The designation (1) or (2) in the column headings refers to the source of the data. Values designated (1) were taken from the list published by Hopfinger.[31] Those denoted by (2) were calculated as described in the text. [b] The parameters used in the calculation of $A(2)_{ij}$ and $B(2)_{ij}$ were as follows: $\alpha(2)_P = 2.80$, $\alpha(2)_N = 1.15$, $\alpha(2)_F = 0.38$, $\alpha(2)_{Cl} = 2.28$, $\alpha(2)_{Br} = 3.34$, $\alpha(2)_I = 5.00$; $N_{eff}(2)$ values were P = 14.10, N = 6.00, F = 7.90, Cl = 16.20, Br = 21.90, I = 26.80; r^0 values (Å) were P = 1.80, N = 1.55, F = 1.47, Cl = 1.75, Br = 1.85, I = 1.98.

in which the interatomic distance was invariant with torsional angle.[30]

Structure IV was examined by 20° incremental torsion of bonds P_1–N_2, N_2–P_2, P_2–N_3, and N_3–P_3 through 360°. The program contained two options. In the first (option a) the "terminal" segment, based on skeletal bonds P_2–N_3, N_3–P_3, and P_3–N_4, was allowed to undergo compensatory torsional energy minimization about bonds P_2–N_3 (ϕ') and N_3–P_3 (ψ') for each conformation generated by the torsion of bonds P_1–N_2 (ϕ) and N_2–P_2 (ψ). The second option (option b), used to generate a ψ,ϕ' map, allowed the segments N_1–P_1–N_2 and N_3–P_3–N_4 to undergo energy minimization by torsion about bonds N_2–P_1 (ϕ) and N_3–P_3 (ψ') respectively for each conformation generated by torsion of bonds N_2–P_2 (ψ) and P_2–N_3 (ϕ'). Again, two-bond interactions, which presumably do not vary with torsional angle changes, were neglected. Structure IV (option a) was compared with structure III to establish that the general pattern of results given by structure III was not in error due to neglect of the longer range interactions.

Potential Energy Calculations. A classical "6–12" Lennard–Jones equation of the form:

$$U_{ij} = (B_{ij}/r_{ij}^{12}) - (A_{ij}/r_{ij}^{6})$$

was used together with a Coulombic term of the type:

$$V_{ij} = (kQ_iQ_j)/(\epsilon r_{ij})$$

No intrinsic torsional potential for the backbone bonds was used. Although π-bond stabilization is believed to exist in phosphazenes,[16a,b] the interaction may be of the dπ–pπ type, involving phosphorus 3d orbitals and nitrogen 2p orbitals. Because of the spherical symmetry and diffuse character of the d-orbital cluster at phosphorus, no significant barrier would be expected. The physical properties of polyphosphazenes tend to confirm this supposition.[16]

The *A* and *B* values used in the Lennard–Jones equation were obtained from the tabulations by Hopfinger[31] (potential No. 1) or were calculated directly from the Pitzer[32] modification of the Slater–Kirkwood equation (potential No. 2). Potential 1 could be used only for the fluoro and chloro derivatives. The equation used for calculation of the *A* terms for potential 2 was:

$$A_{ij} = [\tfrac{3}{2}e(\hbar/m^{1/2})\alpha_i\alpha_j]/C_{ij}$$

where $C_{ij} = (\alpha_i/N_{eff}^{(i)})^{1/2} + (\alpha_j/N_{eff}^{(j)})^{1/2}$. The atomic polarizabilities, α, were obtained from the data by Ketelaar,[33] and the N_{eff} values were obtained by the Scott and Scheraga[34] modification of the method by Pitzer.[32] The *B* terms were calculated from $B_{ij} = A_{ij}R_0^6/2$, where $R_0 = r_i^0 + r_j^0 + 0.20$ Å, the sum of the van der Waals radii modified according to the approach used by Brant, Miller, and Flory.[35] The van der Waals radii values (r^0) were obtained from the tabulation by Bondi.[36] The values used in each case are listed in Table II.

For the Coulombic calculation, the dielectric constant, ε, was fixed at 4.0. This value was based on experimental measurements of the dielectric constant of $(NPCl_2)_3$ and $(NPCl_2)_n$.[37] The conversion constant, *k*, was 332 to express the energy values in kcal/mol. Values for the partial charges, Q_i and Q_j, were estimated by the method of Smyth[38] from the equation $Q = 0.16(X_a - X_b) + 0.035(X_a - X_b)^2$ where *X* is the Pauling electronegativity. The partial charges (*Q*) used were: for $(NPF_2)_n$, +1.12 (P), −0.32 (N), and −0.4 (F); for $(NPCl_2)_n$, +0.70 (P), −0.32 (N), −0.19 (Cl); for $(NPBr_2)_n$, +0.60 (P), −0.32 (N), −0.14 (Br); for $(NPI_2)_n$, +0.48 (P), −0.32 (N), −0.08 (I). The use of molecular orbital methods for the calculation of charge densities was considered inadvisable in view of the multielectron character of the phosphazene system. In spite of the severe approximations inherent in the Coulombic estimates (which, if anything, would overestimate the Coulombic influence), it was found that the Coulombic contributions had only a minimal effect on the energy surfaces.

The Fortran IV programs were arranged to provide three options: an energy surface based on the Lennard–Jones term alone, a surface based on the Coulombic term, or a surface based on the sum of the two. The computations were carried

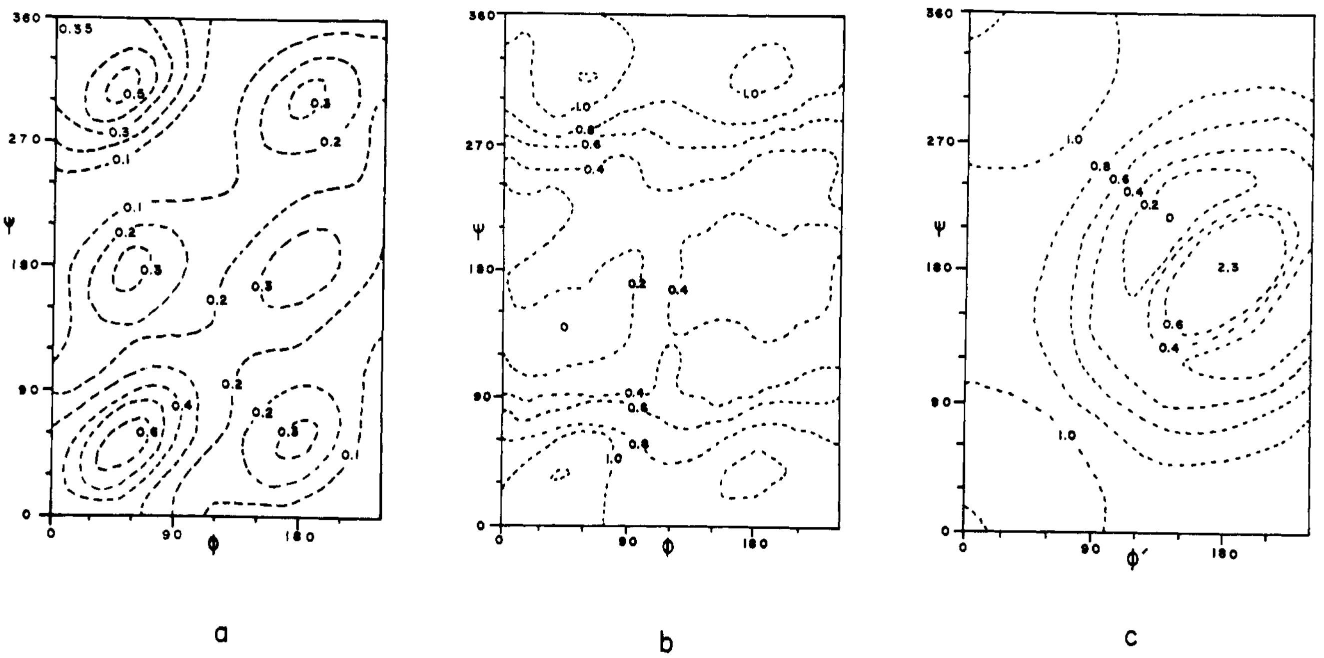

Figure 1. Calculated Lennard–Jones plus Coulombic potential energy surfaces for $(NPF_2)_n$, potential 2: (a) structure III, (b) structure IVa, (c) structure IVb. The contour intervals are 0.1 kcal/mol residue for (a) and 0.2 kcal/mol residue for (b) and (c).

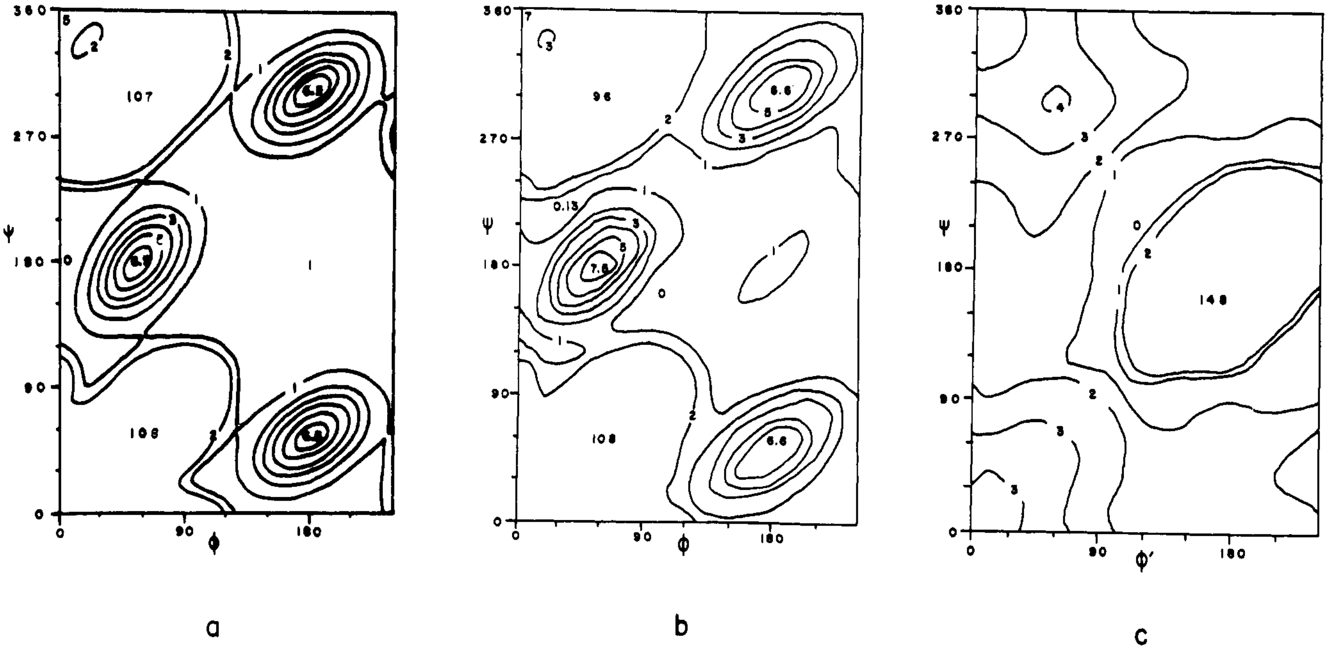

Figure 2. Calculated Lennard–Jones plus Coulombic potential energy surface for $(NPCl_2)_n$, potential 2: (a) for structure III, (b) for structure IVa, (c) for structure IVb. Contour intervals are shown every 1 kcal/mol residue.

out with the use of an IBM 370/168 computer at The Pennsylvania State University.

Interpretation of Energy Maps. The energy surfaces shown in Figures 1–4 generate the trans-trans conformation (as shown in III) at position $\phi = 0°$, $\psi = 0°$ and symmetry related points. Position $\phi = 0°$, $\psi = 180°$ corresponds to the cis-trans planar conformation (structure II). Skeletal torsional motions of ++ type (i.e., "parallel" torsion of two adjacent skeletal bonds) are simulated by movements on the surface from the $\phi = 0°$, $\psi = 0°$ point diagonally upward on the figure toward $\phi = 180°$, $\psi = 180°$. Motions of the +− type (counter rotation) can be followed from position $\phi = 0°$, $\psi = 360°$ diagonally downward toward the bottom right of each figure. The surfaces for structures III and IVb are symmetric about the diagonals; those for structure IVa are centrosymmetric, hence, only slightly more than one half of each surface is shown.

Results and Discussion

Choice of Preferred Models. It was first necessary to eliminate from serious consideration those trial models (Table I) which yielded unacceptably high energies for all conformations or which yielded energy minima that were grossly incompatible with known chain conformations. Slight differences were found between energy surfaces calculated with the use of potentials 1 and 2. Potential 2 yielded steeper barriers but generated slightly lower absolute energy minima. Table I lists the structural parameters chosen for each polymer.

The parameters used for poly(difluorophosphazene) were

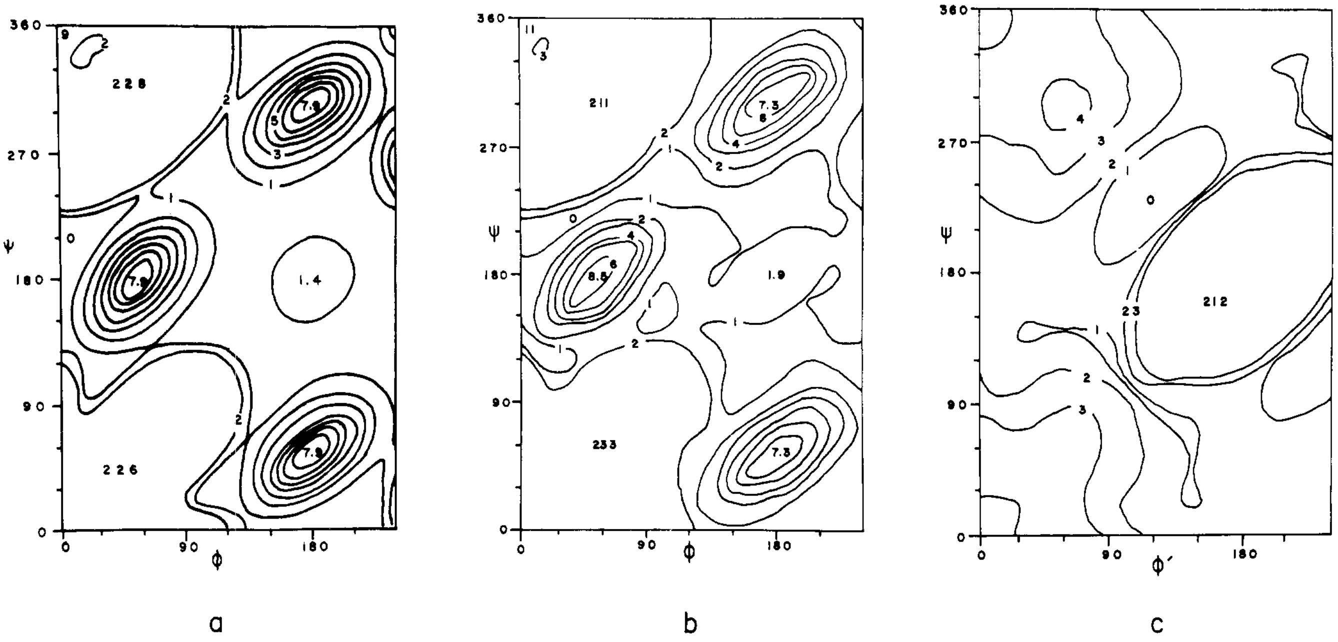

Figure 3. Calculated Lennard–Jones plus Coulombic potential energy surface for $(NPBr_2)_n$, potential 2: (a) for structure III, (b) for structure IVa, (c) for structure IVb. Contour intervals are shown every 1 kcal/mol residue.

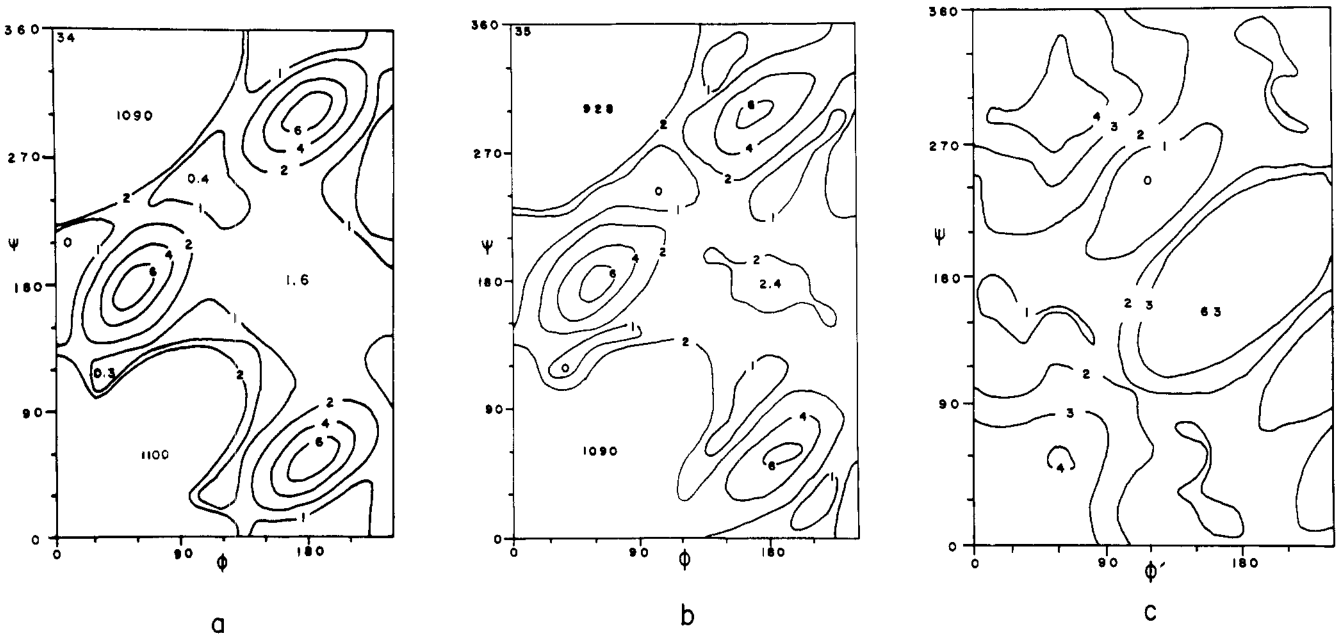

Figure 4. Calculated Lennard–Jones plus Coulombic potential energy surface for the yet-unsynthesized $(NPI_2)_n$, potential 2: (a) for structure III, (b) for structure IVc, (c) for structure IVb.

obtained from a recent x-ray diffraction determination of $(NPF_2)_n$.[12] These values also yielded lower energy minima in trial calculations than did the alternative models. The structural parameters for poly(dichlorophosphazene) were selected on the basis of x-ray crystallographic data for cyclic oligomers,[24-26] from the general trend of P–N bond shortening for larger ring systems, and from preliminary analyses of x-ray fiber diagrams obtained from $(NPCl_2)_n$.[18,39] Moreover, the model chosen generated lower energy minima than the other alternatives and yielded minima at conformations that were compatible with the X-ray diffraction data. The bond angles and bond lengths for poly(dibromophosphazene) again were chosen on the basis of single crystal X-ray data for the cyclic trimer, modified to take into account the P–N–P bond angle widening expected in a linear molecule. The chosen model also yielded the most energetically acceptable surface of all those evaluated. Poly(diiodophosphazene) has not yet been synthesized. Indeed, the cyclic trimer is unknown. The calculations were performed mainly to determine if any intramolecular steric forces could be identified that might destabilize this polymer.

Comparison of Different Structural Approaches. Only minor differences were detected between the surfaces generated from the five-skeletal atom segment (III) and the seven-skeletal atom unit (IVa) (Figures 1–4). Moreover, the calculated barriers (Table III) are quite similar for the two segments. The absolute minimum energy values (Table III) are lower for segments of type IVa than for those derived from III. This simply reflects the fact that the "residue" in IV contains a larger number of atoms. The expected change (by a factor of ~2) is consistent with the data. The exact positions of the minima are less easily identified from the surfaces de-

Table III
Comparison of Conformational Minima, Barrier Heights, and Minimum Energy Values for Model Structures III and IV

Structure		Principal minima[a-c]			Barriers, kcal/residue	Min. energy values,[d] kcal/residue
$(NPF_2)_n$	III	0:180 (0.07)	100:270	0:140 (0.06)	0.05	−34.93
	IVa	20:200 (0.13)	100:220 (0.26)	40:140	0.39	−70.66
	IVb	40:160 (0.84)	140:220		0.90	−70.66
$(NPCl_2)_n$	III	10:210	130:230	120:150	1.01	−16.33
	IVa	40:220 (0.13)	180:240	100:160	0.94	−35.05
	IVb	20:160 (1.21)	120:200		1.42	−35.05
$(NPBr_2)_n$	III	10:210	210:250 (0.37)	110:150 (0.37)	1.04	−13.74
	IVa	40:220	180:240	100:160 (0.34)	1.09	−30.26
	IVb	40:140 (0.91)	120:220		1.35	−30.26
$(NPI_2)_n$	III	10:210 (0.31)	30:110	100:260 (0.43)	0.87	−10.87
	IVa	20:200 (0.59)	40:120	100:240	1.71	−25.69
	IVb	20:160 (0.81)	120:240		1.45	−25.69

[a] Coordinates are listed in the order ϕ:ψ for structures III and IVa and ϕ':ψ for structure IVb. [b] It is important to note that the ϕ,ψ values for structure IV are subject to much greater deviations (estimated at ±10°) because the calculated matrix was at 20° torsional intervals (rather than the 10° for structure III), a restriction dictated by the computational facilities. [c] Values in parentheses indicate the energy (in kcal/residue) of that minimum above that of the lowest minimum. [d] Seven-skeletal residue for IV vs. five-skeletal atom residue for III.

rived from IV because of the lower resolution inherent in the 20° torsional increments. (This restriction was imposed by the limits of the computational system.) Nevertheless, it is clear from Figures 1–4 and from Table III that the primary minima are generated from IVa in the same general regions as those derived from III. Thus, the use of the shorter chain segment (III) provides a satisfactory model for the analysis of more complex phosphazene polymers that cannot be handled at present by the use of the seven-skeletal atom approach (see following paper).

The surfaces generated from IVb (ψ,ϕ' plots) are also shown in Figures 1–4. These explore the ability of the polymer to assume or avoid cis-cis (ψ = 180°, ϕ' = 180°) or related conformations.

Minimum Energy Conformations. The chain conformation assumed by a crystalline high polymer generally corresponds to a minimum in the nonbonding potential energy surface.[40] Table III lists the conformational minima calculated for the four polymers for structures III, IVa, and IVb.

For $(NPF_2)_n$, structures III and IVa generated a minimum at or near the ϕ = 0°, ψ = 180° (cis-trans planar) conformation found from the low-temperature x-ray diffraction analysis. (This was most noticeable when potential 1 was employed with structure III.) The ψ,ϕ' plot (Figure 1c) revealed an additional minimum at ψ = 220°, ϕ' = 140°. However, it must be stressed that these minima are really shallow depressions in a broad area of low potential in which energy differences do not exceed 0.6 kcal/mol residue. Although intermolecular forces undoubtedly exert an additional influence, the flatness of the intramolecular surface may explain the facile conversion from one conformer to another at low temperatures.[12]

The energy minima calculated for $(NPCl_2)_n$ are shown in Table III. Structure III generated a marked minimum at or near the cis-trans planar (ϕ = 0°, ψ = 180°) position. This conformation corresponds to the one deduced from x-ray diffraction repeat distance and intensity analysis data.[18,39] All models provided an additional broad, circular-shaped low-energy well corresponding to conformations displaced slightly from the cis-cis (ϕ = 180°, ψ = 180°) position. Stretching of the polymer or the presence of intermolecular packing forces in the microcrystalline state may favor the occupation of the cis-trans planar minimum rather than the "helical" well.

Structures III and IVa for poly(dibromophosphazene) generated a minimum energy conformation near position ϕ = 10°, ψ = 210° (a slightly distorted cis-trans planar arrangement), and a broad circular, low-energy plateau that corresponds to a range of spiral helical conformations. The results suggest that, although a cis-trans planar structure should be preferred, spiral helical conformations are also accessible. Poly(diiodophosphazene), if it can be synthesized, would be expected to behave similarly.

The maps for $(NPCl_2)_n$, $(NPBr_2)_n$, and $(NPI_2)_n$ (structure IVb) indicate that the cis-cis (ψ = 180°, ϕ' = 180°) conformation is unfavorable due to interactions of the terminal groups. However, a slight distortion to ψ = 220°, ϕ' = 120° generates a potential energy minimum for these polymers and for $(NPF_2)_n$. Secondary minima in the ψ,ϕ' plots are noted for a distorted cis-trans planar conformation (ψ = 160°, ϕ' = 20°).

Barrier Heights. Table III lists calculated torsional barriers. The values quoted represent the barrier encountered in following the minimum energy path when a bond undergoes 360° torsion with minimal compensation on the part of the adjacent bonds. The barriers found for poly(difluorophosphazene) (structure III) are negligibly small (0.07 or 0.05 kcal/mol residue for potentials 1 and 2, respectively). For structure IV, the barrier was less than 0.4 kcal/mol residue. In poly(dichlorophosphazene) the torsional barrier is very sensitive to the P–N–P angle. As the angle was widened from 120 to 135°, the calculated barrier dropped from 2–6 kcal to less than 0.5 kcal/mol residue. For the preferred model, the barrier height was calculated to be approximately 0.9 kcal/mol residue for structures III and IV. The barrier in poly(dibromophosphazene) was calculated to be approximately 1.1 kcal/mol residue for the most plausible model. The calculated barrier for poly(diiodophosphazene) was slightly higher (1.5 kcal/mol residue). Thus, a rough parallel exists between the glass transition temperatures of the fluoro, chloro, and bromo derivatives (−95, −63, and −15°, respectively) and the small increase in the calculated barrier height.

Chain Flexibility. The flexibility of the chain (and, thereby, the flexibility or elasticity of the material) depends on the differences in energy between low-lying minima, on the breadth of the principal wells, and probably on the barrier to major torsional backbone motions. The poly(dihalophosphazenes) are especially suited to an analysis of chain flexibility because the influence of side group changes can be monitored with particular ease.

Poly(difluorophosphazene) has one of the lowest glass transition temperatures known. Moreover, this polymer undergoes facile conformational changes in the rubbery state at low temperatures.[12] The energy surfaces calculated in this work suggest that the molecule can undergo broad conformational changes involving 360° torsion of adjacent skeletal bonds without encountering barriers greater than 0.4 kcal/mol residue. Indeed, there appears to be little intramolecular inducement for this polymer to prefer any one conformation over another. Even when alternative minima appear in the calculations, the energy difference between them is generally less than 0.3 kcal/mol residue. Thus, it must be assumed that the preference for one conformation or another is determined mainly by slight differences in *inter*molecular packing forces.

Poly(dichlorophosphazene) can also apparently undergo broad conformational changes without encountering barriers greater than 1.0 kcal/mol residue (Figure 2). This conformational flexibility is especially characteristic of the spiral helical forms represented by the broad circular well surrounding the cis-cis peak. This well is also found for poly(dibromophosphazene) (Figure 3), but the range of accessible conformations is more restricted. These facts may explain the differences in glass transition temperatures and perhaps also the observation that poly(dibromophosphazene) is a less flexible elastomer than the fluoro or chloro derivatives. The surfaces for the iodo derivative (Figure 4) suggest that this polymer should show similar physical properties to the bromo derivative.

Thermal Stability. Finally, it is instructive to examine the relationship of the energy surfaces calculated in this work to the practical problems of thermal stability and ring-polymer equilibria.[41] Although the calculated minimum enthalpy values (Table III) for the fluoro, chloro, bromo, and iodo derivatives increase in the order −35, −16, −13, and −11 kcal/mol residue for structure III, these values neglect the near-neighbor interactions which do not vary with conformational changes. If the near-neighbor interactions are included, the energies are in the region of +114, +72, +46, and +25 kcal/mol residue. However, these nonbonding terms are over-ridden by the change in P-halogen *bond* energy terms, which are estimated to be in the region of −468, −305, −252, and −176 kcal/mol residue, respectively. Hence the predicted order of over-all stability should be $(NPF_2)_n > (NPCl_2)_n > (NPBr_2)_n > (NPI_2)_n$.

Acknowledgment. We thank the Army Research Office for the support of this work.

References and Notes

(1) This paper is part 28 in a series on phosphorus-nitrogen compounds.
(2) Part 27: H. R. Allcock and D. B. Patterson, *Inorg. Chem.*, in press.
(3) H. R. Allcock and R. L. Kugel, *J. Am. Chem. Soc.*, 87, 4216 (1965).
(4) H. R. Allcock, R. L. Kugel, and K. J. Valan, *Inorg. Chem.*, **5**, 1709 (1966).
(5) H. R. Allcock and R. L. Kugel, *Inorg. Chem.*, **5**, 1716 (1966).
(6) S. H. Rose, *J. Polym. Sci., Part B*, **6**, 837 (1968).
(7) H. R. Allcock, W. J. Cook, and D. P. Mack, *Inorg. Chem.*, **11**, 2584 (1972).
(8) H. R. Allcock and G. Y. Moore, *Macromolecules*, **5**, 231 (1972).
(9) G. Allen, C. J. Lewis, and S. M. Todd, *Polymer*, **11**, 31 (1970).
(10) G. L. Hagnauer and N. S. Schneider, *J. Polym. Sci., Part A2*, **10**, 699 (1972).
(11) R. E. Singler, G. L. Hagnauer, N. S. Schneider, B. R. LaLiberte, R. E. Sacher, and R. W. Matton, *J. Polym. Sci.*, **12**, 433 (1974).
(12) H. R. Allcock, R. L. Kugel, and E. G. Stroh, *Inorg. Chem.*, **11**, 1120 (1972).
(13) H. R. Allcock and W. J. Cook, *Macromolecules*, **7**, 284 (1974).
(14) H. R. Allcock, G. Y. Moore, and W. J. Cook, *Macromolecules*, **7**, 571 (1974).
(15) H. R. Allcock, J. E. Gardner, and K. M. Smeltz, *Macromolecules*, **8**, 36 (1975).
(16) For reviews of this subject, see: (a) H. R. Allcock, "Phosphorus-Nitrogen Compounds", Academic Press, New York, N.Y., 1972; (b) H. R. Allcock, *Chem. Rev.*, **72**, 315 (1972); (c) H. R. Allcock, *Chem. Br.*, 118 (April, 1974); (d) D. P. Tate, *J. Polym. Sci., Polym. Symp.*, **No. 48**, 33 (1974); and (e) R. E. Singler, N. S. Schneider, and G. L. Hagnauer, *Polym. Eng. Sci.*, **15**, 321 (1975).
(17) S. H. Bishop and I. H. Hall, *Br. Polym. J.*, **6**, 193 (1974).
(18) E. Giglio, F. Pompa, and A. Ripamonti, *J. Polym. Sci.*, **59**, 293 (1962).
(19) H. R. Allcock, R. L. Kugel, G. F. Konopski, and E. G. Stroh, *Chem. Commun.*, 985 (1970).
(20) D. Cordischi, A. D. Site, A. Mele, and P. Porta, *J. Macromol. Chem.*, **1**, 219 (1966).
(21) See ref 16a, Appendix 1 and Chapters 2 and 3.
(22) M. W. Dougill, *J. Chem. Soc.*, 3211 (1963).
(23) H. McD. McGeachin and F. R. Tromans, *J. Chem. Soc.*, 4777 (1961).
(24) G. J. Bullen, *J. Chem. Soc. A*, 1450 (1971).
(25) A. J. Wagner and A. Vos, *Acta Crystallogr., Sect. B*, **24**, 707 (1968).
(26) A. W. Schlueter and R. A. Jacobson, *J. Chem. Soc. A*, 2317 (1968).
(27) H. Zoer, D. A. Koster, and A. J. Wagner, *Acta Crystallogr., Sect. A*, **25**, S 107 (1969).
(28) E. Giglio and R. Puliti, *Acta Crystallogr.*, **22**, 304 (1967).
(29) Y.C. Leung and J. Waser, *J. Phys. Chem.*, **60**, 539 (1956).
(30) Some preliminary computations to monitor the effects of parameter changes on structure III were made with a rapid, inexpensive program developed by J. E. Lehnsen, American Cyanamid Co., Stamford, Conn. This program calculated distances N_1–N_3, N_1–R_3, N_1–R_4, R_1–N_3, R_2–N_3, R_1–R_3, R_1–R_4, R_2–R_3, and R_2–R_4 but neglected interactions such as N_1–R_1 or N_1–R_2 and did not include the phosphorus atoms in the computation. However, the data reported in this paper were obtained with the more comprehensive program described in the text.
(31) A. J. Hopfinger, "Conformational Properties of Macromolecules", Academic Press, New York, N.Y., 1973, p 47.
(32) K. S. Pitzer, *Adv. Chem. Phys.*, **2**, 59 (1959).
(33) J. Ketelaar, "Chemical Constitution", Elsevier, New York, N.Y., 1958, p 91.
(34) R. A. Scott and H. A. Scheraga, *J. Chem. Phys.*, **42**, 2209 (1965).
(35) D. A. Brant, W. G. Miller, and P. J. Flory, *J. Mol. Biol.*, **23**, 47 (1967).
(36) A. Bondi, *J. Phys. Chem.*, **68**, 441 (1964).
(37) H. R. Allcock and R. J. Best, *Can. J. Chem.*, **42**, 447 (1964).
(38) C. P. Smyth, "Dielectric Behavior and Structure", McGraw-Hill, New York, N.Y., 1955, pp 289–311.
(39) K. H. Meyer, W. Lotmar, and G. W. Pankow, *Helv. Chim. Acta*, **19**, 930 (1936).
(40) P. DeSantis, E. Giglio, A. M. Liquori, and A. Ripamonti, *J. Polym. Sci., Part A*, **1**, 1383 (1963).
(41) It should be noted that the calculated energy of the cis-cis conformation (ϕ or $\phi' = 180°$, $\psi = 180°$) provides a rough measure of the stability of the planar form of the cyclic trimer. Peaks were detected at this position for the chloro, bromo, and iodo models, and these presumably represent N_1–N_3 or N_1–N_4 nonbonding repulsions. These repulsions can be relieved by a slight twist of the skeleton, and this may explain why both $(NPCl_2)_3$ and $(NPBr_2)_3$ are slightly puckered in the crystalline state. The fluoro derivative, $(NPF_2)_3$, is planar, and the energy surface for this polymer shows virtually no repulsion at the cis-cis conformation (Figure 1c).